

**Intelligent ZIF-8-Gated Polydopamine Nanoplatfom for in vivo Cooperatively
Enhanced Combinational Phototherapy**

Jie Feng^{‡, a, b} Wenqian Yu^{‡, a} Zhen Xu,^a Fuan Wang^{*a}

^a Key Laboratory of Analytical Chemistry for Biology and Medicine (Ministry of Education), College of Chemistry and Molecular Sciences, Wuhan University, Wuhan 430072, P. R. China

^b College of Chemistry, Chemical Engineering and Materials Science, Collaborative Innovation Center of Functionalized Probes for Chemical Imaging in Universities of Shandong, Key Laboratory of Molecular and Nano Probes, Ministry of Education, Shandong Normal University, Jinan 250014, P. R. China

* To whom correspondence should be addressed. E-mail: fuanwang@whu.edu.cn

Table of Contents

Experimental Section	S1-S7
Fig. S1 The photo images of different nanomaterials.....	S8
Fig. S2 TGA curves of ZIF-8, PZ, PMZ and PMCZ.....	S9
Fig. S3 FTIR spectrum of free CAT, MB, PDAs, ZIF-8 and PMCZ.....	S10
Fig. S4 Quantification of BSA by UV- <i>vis</i> absorbance.....	S11
Fig. S5 Fluorescence spectra-derived standard work curves of MB.....	S12
Fig. S6 UV- <i>vis</i> absorption spectra PDA, MB, PZ and PMCZ.....	S13
Fig. S7 Photothermal performances analysis.....	S14
Fig. S8 Temperature changes of photoirradiated PMCZ.....	S15
Fig. S9 Cell viability of PMCZ.....	S16
Fig. S10 IC50 values for different treatments.....	S17
Fig. S11 Demonstration of the wavelength-specific PTT and PDT effects.....	S18
Fig. S12 Hematology analysis.....	S19
Fig. S13 Quantification of intracellular Zn ²⁺ ions by ICP-AES.....	S20
Fig. S14 <i>Ex vivo</i> fluorescence images of major organs.....	S21
Fig. S15 Temperature curves of tumor sites.....	S22
Fig. S16 Western blot assays.....	S23
Fig. S17 H&E staining of major organs.....	S24
Fig. S18 Body weights of mice.....	S25

Experimental Section

Materials

Zinc nitrate hexahydrate ($\text{Zn}(\text{NO}_3)_2 \cdot 6\text{H}_2\text{O}$, 98%), 2-methylimidazole (99%), sodium phosphate monobasic (NaH_2PO_4 , 98%), sodium phosphate dibasic (Na_2HPO_4 , 99%), catalase (from bovine liver), sodium acetate (NaAc, 99%), trizma hydrochloride (99%), trizma base (99%), L-glutathione reduced (GSH, 98%) and 1,3-diphenylisobenzofuran (DPBF, 97%) were purchased from Sigma-Aldrich. Methylene blue trihydrate (MB), ethanol absolute (AR) and acetic acid (HAc, AR) were purchased from Sinopharm Chemical Reagent Co., Ltd. Dopamine hydrochloride (98%) were purchased from Aladdin. Thiazolyl blue (98%), Trypsin-EDTA (0.25%), Pen Strep (100 \times) (Pan 10000 U/mL, Str 10000 $\mu\text{g}/\text{mL}$, PBS 0.01 mol/L) and paraformaldehyde (4%) were purchased from Beijing Dingguo Changsheng Biotechnology Co., Ltd. DMEM/HIGH GLUCOSE (L-Glutamine 4.00 mM, Glucose 4500 mg/L) and phosphate buffer saline (1 \times) (0.0067 M, none of Calcium and Magnesium) were purchased from HyClone. 2-(4-amidinophenyl)-6-indolecarbamide dihydrochloride (DAPI) and reactive oxygen species detection kit (DCFH-DA) were purchased from Beyotime Biotechnology Co., Ltd. Tis (4,7-diphenyl-1,10-phenanthroline) ruthenium (II) dichloride $[\text{Ru}(\text{dip})_3]\text{Cl}_2$ was purchased from Alfa Aesar (China) Chemicals, Ltd. Fetal bovine serum (Australian origin) was purchased from PAN-Biotech. Calcein-AM/PI double stain kit was purchased from Shanghai Yeasen Biotechnology Co., Ltd.

Characterization

Instruments for characterization of materials are Smart lab 9 kW X-ray diffractometer (Rigaku, Japan), Nicolet iS10 FT-IR spectrometer (Thermo Fisher Scientific, USA), Cary Eclipse Fluorescence Spectrophotometer (Agilent Technologies, USA), UV-2600 UV-Vis Spectrophotometer (Shimadzu, Suzhou), Zeta sizer Nano-ZS90 (Malvern, UK), Field Emission Scanning Electron Microscopy (SEM) (Zeiss Merlin Compact, Germany) and HT-7700 Transmission Electron Microscopy (TEM) (Hitachi, Japan). Instruments for cell experiments are Revolution XD spinning-disk confocal microscope (Andor, UK), Laser instrument (Hi-Tech Optoelectronics Co., Ltd. China), Multiskan GO (Thermo Fisher Scientific, USA) and BD FACS Verse flow cytometry (BD Medical

Technology, China).

Synthesis of polydopamine nanoparticles (PDAs). PDAs were synthesized from a mixture of $\text{NH}_3 \cdot \text{H}_2\text{O}$ (3.0 mL, 28%-30%), ethanol (40 mL), H_2O (90 mL) by a previously reported procedure with slight modification. The mixture was further mildly stirred for 30 min at 30 °C before dopamine hydrochloride (0.5 g DA, 10 mL H_2O aqueous solution) was injected into the mixture, and then stirred for 24 h. PDAs were collected by centrifugation at 10000 rpm for 20 min and washed several times with water. The precipitate was finally dispersed in water (4 mg/mL) for further used and stored at 4 °C.

Synthesis of PDAs-ZIF-8 (PZ). 2-Methylimidazole (2-MIM, 1 mL, 1.32 M) was added into PDAs (1.0 mL, 400 $\mu\text{g}/\text{mL}$) under stirred. One minute later, $\text{Zn}(\text{NO}_3)_2 \cdot 6\text{H}_2\text{O}$ (1 mL, 24 mM) was injected into the above mixture quickly, and stirred for 5 minutes, then placed for 3 h at room temperature. The product was collected by centrifugation at 12000 rpm for 30 min and washed with water for several times.

One-pot Synthesis of PDAs-MB-CAT-ZIF-8 (PMCZ). Firstly, 2-methylimidazole (2-MIM, 1 mL, 1.32M) and MB (1 mg) was mixed together in water, then the mixture was added into PDAs (1.0 mL, 400 $\mu\text{g}/\text{mL}$) under stirred. After 1 min, the mixture of $\text{Zn}(\text{NO}_3)_2 \cdot 6\text{H}_2\text{O}$ (1 mL, 24 mM) and 5 mg catalase was added quickly, continued stirring for 5 minutes. The reaction was placed for 3 h at room temperature. As a control group, PMZ was synthesized without catalase. The final product was collected by centrifugation and dried in vacuum.

BCA protein Assay. The concentration of catalase was determined by BCA reagents (purchased from Beyotime) in a standard method. The protocol was carried out based on the supplier.

Photothermal performances analysis. For measuring the photothermal conversion performance of PMCZ, 1 mL aqueous dispersion of PMCZ with different concentrations (0, 25, 50, 100, 200 $\mu\text{g}/\text{mL}$) were introduced in a quartz cuvette and irradiated with an 808 nm NIR laser at a power density of 2 W/cm^2 for 500 s, respectively. A thermocouple probe with an accuracy of 0.1 °C was inserted into the PMCZ aqueous solution perpendicular to the path of the laser. The temperature was

recorded every 10 s by a digital thermometer with a thermocouple probe.

Extracellular O₂ evolution in response to H₂O₂. For detection of extracellular O₂, the commercial chemical probe RDPP was used by detecting its fluorescence intensity at 455 nm excitation wavelength. In a total volume 500 μ L, RDPP (25 μ L, 10 mM) was added to PMCZ (25 μ L, 4 mg/mL) in water solution (445 μ L). After the addition of H₂O₂, fluorescence spectrum was recorded with fluorescence spectrophotometer. As the control, the groups of PDAs, PZ and PMZ were detected with the same method, respectively.

Intracellular O₂ evolution in response to H₂O₂. HeLa cells (1×10^5) were seeded in confocal dishes for 24 h. Then cells were washed with PBS for three times and incubated with RDPP (5 μ M) for 4 h at 37 °C. Subsequently, cells incubated with PMCZ (50 μ g/mL) for 4 h. The fluorescence images were obtained at 488 nm excitation using a confocal imaging system.

Extracellular ¹O₂ detection. The extracellular ¹O₂ was determined by DPBF, a ¹O₂ probe whose absorption intensity can be strongly decreased by ¹O₂. Briefly, DPBF (15 μ L, 10 mM) and PMCZ (50 μ g/mL) were mixed with PBS-ethanol (v/v = 4:6) mixed solution (pH 7.4). After added with H₂O₂, the sample was irradiated under 660 nm laser for 6 min. The loss of UV absorption intensity of DPBF at 410 nm was recorded at a certain time. As a control group, the solution without H₂O₂ at pH 7.4 was served. To further study the *in vitro* acidic H₂O₂-enhanced ¹O₂ generation, DPBF (15 μ L, 10 mM) and PMCZ (50 μ g/mL) were mixed with PBS-ethanol (v/v = 4:6) mixed solution (pH 5.0) instead of pH 7.4.

Intracellular ¹O₂ detection. HeLa cells were incubated with PMCZ (50 μ g/mL) for 4 h and washed three times by PBS. Then DPBF (10 μ M) was further incubated with cells for 30 min at 37 °C. Afterwards, cells were irradiated under 660 nm laser for 3 min. Finally, the fluorescence images were obtained at 488 nm excitation using a confocal imaging system. In order to study the intracellular acidic H₂O₂-enhanced ¹O₂ generation, the group of PMZ was detected with the same method.

Cellular uptake study. To evaluate the cell uptake ability of PMCZ (50 μ g/mL), HeLa cells were pre-seeded in confocal dishes for 24 h in CO₂ incubator at 37 °C. After 4 h

incubation, the loaded cells were washed several times with PBS to remove the residual materials. After fixed with 4% paraformaldehyde for 15 min at 4 °C and then washed with PBS for three times, cells were stained with DAPI for 15 min and finally imaged.

Photothermal and photodynamic therapy. HeLa cells were pre-plated in 96-well plates (1×10^4 cells per well) and cultured overnight. Cells were incubated with a series of concentrations of PMCZ under 37 °C within 5% CO₂. After 4 h, the PTT group was under 808 nm laser irradiation (2 W/cm²) for 3 min, while the PDT group was under 660 nm laser irradiation (100 mW/cm²) for 3 min. To verify the combined PDT and PTT effect at the cellular level, cells were irradiated by 660 nm laser and then 808 nm laser. After illumination, the cells were incubated for another 24 h, then cellular viability was evaluated by standard MTT assay.

The live/dead cell staining assay was carried out on HeLa cells using Calcein-AM/PI double stain kit. Cells were first incubated with PMCZ for 4 h and washed three times by PBS. Subsequently, the cells were exposed under laser and then medium was replaced with con-staining reagent. The fluorescence images were obtained at 488 nm excitation (for calcein AM) and 543 nm excitation (for PI) using a confocal imaging system.

The flow cytometry assay was carried out to evaluate the cytotoxicity of PDT and PTT. The cells were incubated with PMCZ for 4 h, then under 808 nm or 660 nm laser irradiation for 5 min. After incubated for another 24 h, the cells were containing with Annexin V-FITC/PI for 15 min and analyzed by flow cytometry.

Animal tumor xenograft models. All the animal experiments were performed based on the Principles of the Administration of Affairs Concerning Experimental Animals. The animal protocols used in this study were approved by The Institutional Animal Use and Care Committee of Wuhan University of China. HeLa tumor model was established by subcutaneous injection about 1×10^6 cells (dispersed in PBS) into the BABL/c-nude mice (4-6 weeks old). The tumor assays would be carried out when the tumor volumes reached to 80-100 mm³. The tumor volume (V) was determined as the reported method, $V = (W^2 \times L) / 2$ (L, length; W, width).

***In vivo* Fluorescence imaging.** The fluorescence imaging *in vivo* was performed on

CRi maestro small animal imaging system. 100 μ L PMCZ or MB was injected into the HeLa bearing-mice *via* tail vein at a consistent concentration of MB. After the last time points, all mice were sacrificed and the major organs were collected for fluorescence imaging.

***In vivo* photothermal imaging.** PMCZ (50 μ L, 800 μ g/mL) was injected into the mice. As the control, PBS was injected into another mice. The power density of 808 nm laser used was 1 W/cm². IR thermal camera was utilized to monitor the temperature change and quantified the temperature by the BM-IR software.

***In vivo* photothermal therapy and photodynamic therapy.** The mice were randomly divided into six groups (n \geq 4) and treated with: group 1, PBS (50 μ L); group 2, PMCZ (50 μ L, 800 μ g/mL); group 3, PMCZ (50 μ L, 800 μ g/mL) with 660 nm laser irradiation, PMCZ+PDT; group 4, PMCZ (50 μ L, 800 μ g/mL) with 808 nm laser irradiation, PMCZ+PTT; group 5, PMZ (50 μ L, 800 μ g/mL) with 660 nm laser irradiation and 808 nm laser irradiation, PMZ+PDT+PTT; 6, PMCZ (50 μ L, 800 μ g/mL) with 660 nm laser irradiation and 808 nm laser irradiation, PMCZ+PDT+PTT. After 12 h treated, PDT was carried out on group 3 treated with 660 nm laser irradiation for 5 min at the laser power density of 1 W/cm². PTT was carried out on group 4 treated with 660 nm laser irradiation for 5 min at the laser power density of 1 W/cm². Combination of PDT and PTT were carried out on group 5 and group 6. The two groups were treated with 660 nm laser irradiation for 5 min at the laser power density of 1 W/cm² and then 808 nm laser irradiation for 5 min at the laser power density of 1 W/cm². The tumor volumes and the body weights were recorded every other day and for 14 days totally (day 0, 2, 4, 6, 10, 12 and 14). After the last day treatment, 6 mice (one mouse per group) were sacrificed and cancer tissues were got for histological analysis.

***In vivo* toxicity evaluation.** After 14-day treatment, all mice were sacrificed and their blood and organs were collected. The blood cells were used for Hemolysis Test. The blood cells were incubated with PMCZ at 37 °C for 30 min, and then the samples were centrifuged to detect the hemolysis. The organs were stained with H&E and detected as described above.

HeLa tumor-bearing mice tail vein injection with PMCZ (160 μ L, 2 mg/mL).

Subsequently, all treated mice were sacrificed, followed the tissues were taken out and weighed. In order to digest these tissues, the mixture of HNO₃ and H₂O₂ (volume ratio=1:2) were added into the solution and kept the reaction temperature higher than 200 °C. Then ICP-MS were carried out to analyze the Zn standard solutions with different concentrations (0, 0.5, 1, 5, 10, 50, and 100 µg/mL), and the content of Zn in the prepared solution. The amount of PMCZ was finally calculated by normalizing to percentages of injected dose per gram of tissue (%ID/g).

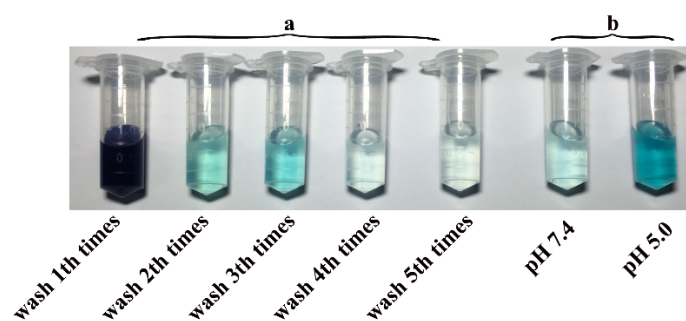


Fig. S1 The photo images of PDAs-MB-CAT-ZIF-8 (PMCZ, 50 $\mu\text{g}/\text{mL}$) after certain round of washing times (a). The corresponding photo images of the supernatant of PMCZ (PMCZ, 50 $\mu\text{g}/\text{mL}$) that was reacted in pH 7.4 and pH 5.0 (b).

The prepared PMCZ was dissolved in 1 mL of water solution. Subsequently, the supernatant obtained from centrifugation was collected for photograph. Repeated this procedure for five times until the supernatant color was clear and transparent. To study the drug release experiment under different pH conditions, PMCZ (50 $\mu\text{g}/\text{mL}$) was dispersed in 1 mL of PBS solution at pH 7.4 and 5.0, respectively. After reaction for 30 min, the supernatant was collected by centrifugation for photograph.

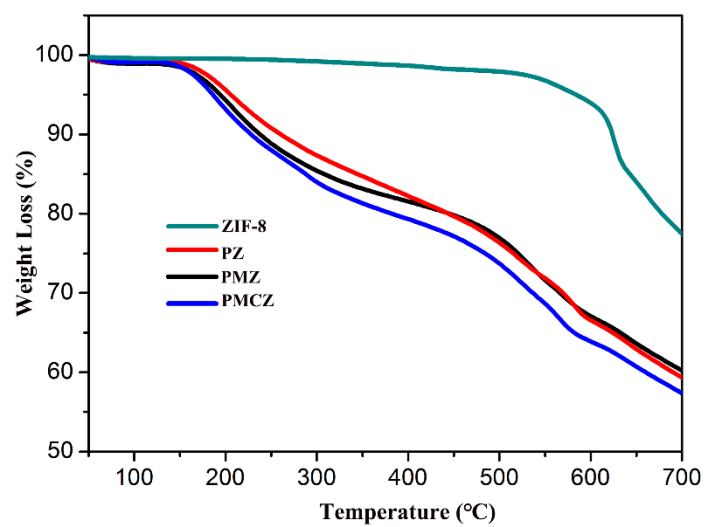


Fig. S2 TGA curves of ZIF-8, PDAs-ZIF-8 (PZ, 50 $\mu\text{g/mL}$), PDAs-MB-ZIF-8 (PMZ, 50 $\mu\text{g/mL}$) and PMCZ (50 $\mu\text{g/mL}$).

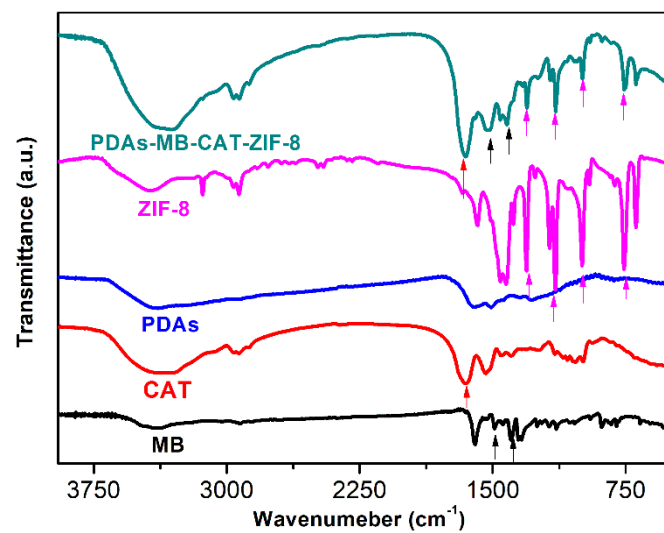


Fig. S3 FT-IR spectrum of free CAT, MB, PDAs, ZIF-8 and PMCZ.

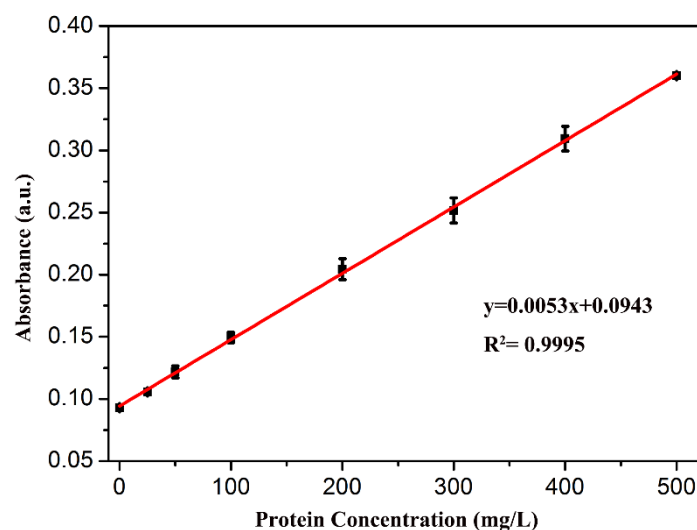


Fig. S4 Linear relationships between UV-vis absorbance and BSA concentration.

In detail, bovine serum albumin (BSA) standards were firstly prepared as manufacturer's instructions. Then a series of BCA working reagent (WR) with increasing BCA was prepared with varying concentrations of standards present in 0, 0.025, 0.05, 0.1, 0.2, 0.3, 0.4 and 0.5 mg/mL. The volumes of all WR solutions were kept constant by adding pure water so that only the BCA concentration varied. Subsequently, the supernatant obtained from centrifugation and washed with H₂O in the above process of synthesis was collected, 20 μ L of the supernatant was added into the WR solutions. After leaving the reaction mixture at 37 °C for 30 minutes, the absorbance at wavelength 562 nm was measured by microplate reader. Finally, the protein concentration of the sample was calculated according to the standard curve and the volume of the used sample. The CAT loading capacity was about 3.4%.

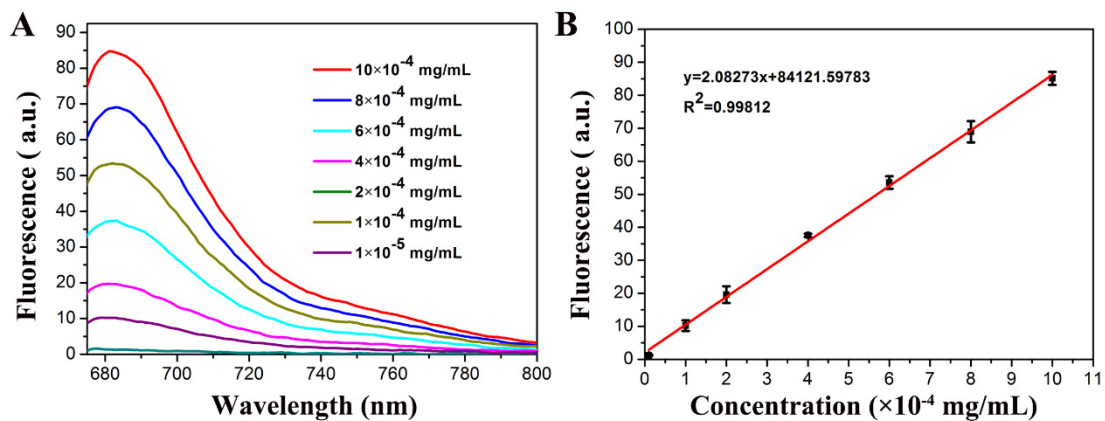


Fig. S5 (A) The fluorescence spectra of MB in water at various concentrations. (B) The calibration curve of MB at 681 nm. The loading amount of MB for PMCZ was quantified by reading characteristic emission peak of MB at 681 nm. According the following equation, the MB loading capacity was calculated: Loading capacity (%) = $(M - M_1) / M_2 \times 100\%$, where M represents the initial feeding amount of MB, M_1 represents the MB content in the supernatant, and M_2 represents the mass of PMCZ. MB loading efficiency were calculation to 5%.

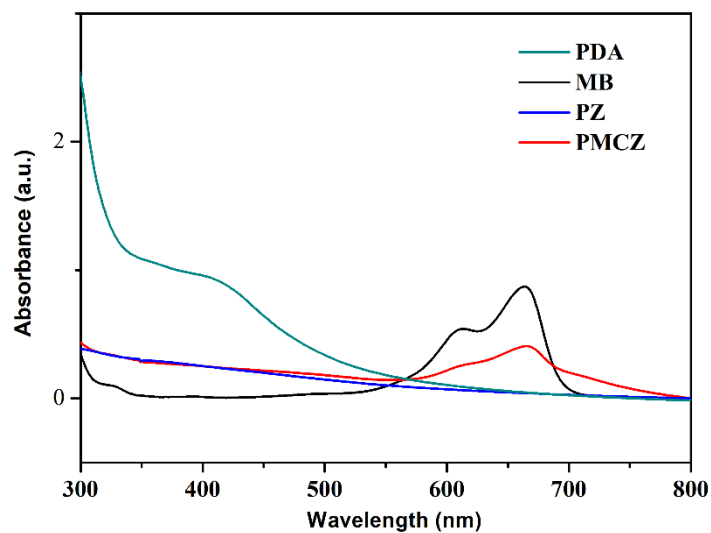


Fig. S6 UV-vis absorption spectra of PDA, MB, PZ and PMCZ. For measuring the UV-vis absorption spectra of different samples, the samples were firstly dispersed in water. Then the UV-vis spectra were recorded on a UV-2600 UV-Vis Spectrophotometer (Shimadzu, Suzhou). Excitation and emission were set to the same wavelength and scanned from 300 nm to 800 nm.

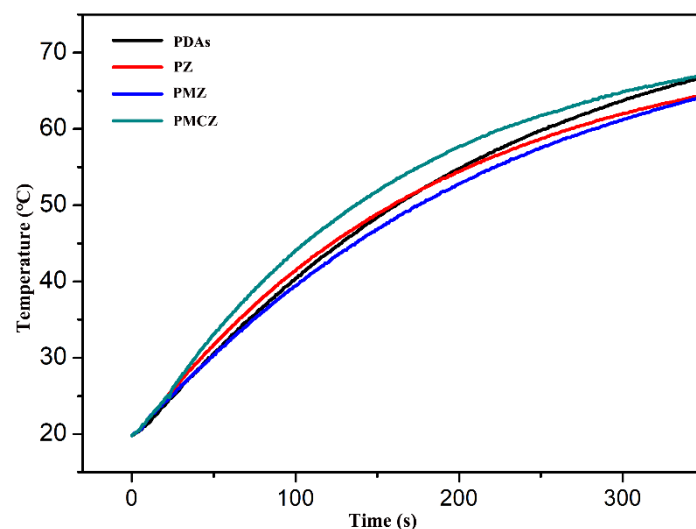


Fig. S7 Temperature rising curves of different samples (ZIF-8, PZ, PMZ and PMCZ, 200 $\mu\text{g/mL}$) under 808 nm irradiation (2 W/cm^2) for 300 s.

To analyze the photothermal performance of different samples, 1 mL aqueous dispersion of ZIF-8, PZ, PMZ and PMCZ with concentration of 50 $\mu\text{g/mL}$ were introduced in a quartz cuvette and irradiated with an 808 nm NIR laser at a power density of 2 W/cm^2 for 350 s, respectively. A thermocouple probe with an accuracy of $0.1 \text{ }^\circ\text{C}$ was inserted into the above aqueous solution perpendicular to the path of the laser. The temperature was recorded every 10 s by a digital thermometer with a thermocouple probe. A similar temperature change was obtained for both of PMCZ and PDAs, indicating that ZIF-8 did not influence the photothermal effect of PDAs.

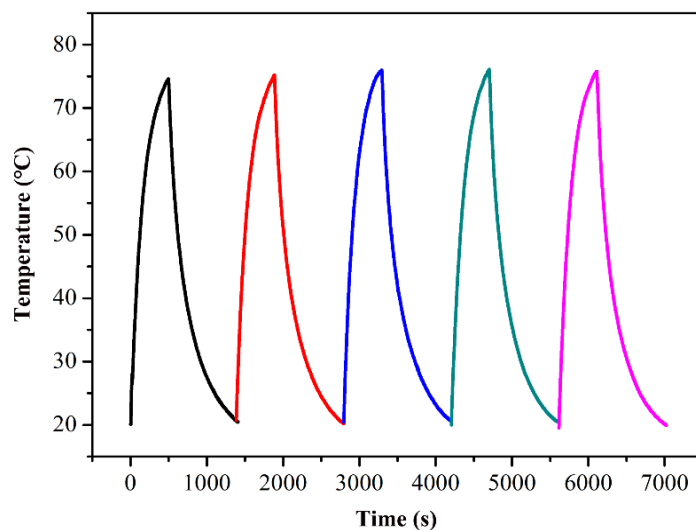


Fig. S8 Temperature change curves of PMCZ (200 $\mu\text{g/mL}$) during five cycles of 808 nm laser irradiation (2 W/cm^2) with on/off states. To evaluate the NIR stability of PMCZ, PMCZ (200 $\mu\text{g/mL}$) were irradiated for 500 s at a power density of 2 W/cm^2 and then the laser was turned off. This procedure was repeated for five times to assess the photostability of PMCZ.

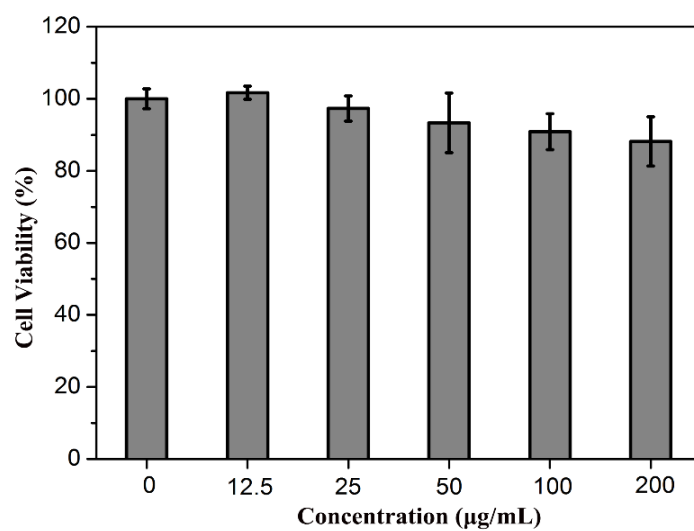


Fig. S9 Cell viability of PMCZ on HeLa cells. The HeLa cells were incubated with different concentrations of PMCZ (0, 12.5, 25, 50, 100, 200 µg/mL) for 4 h.

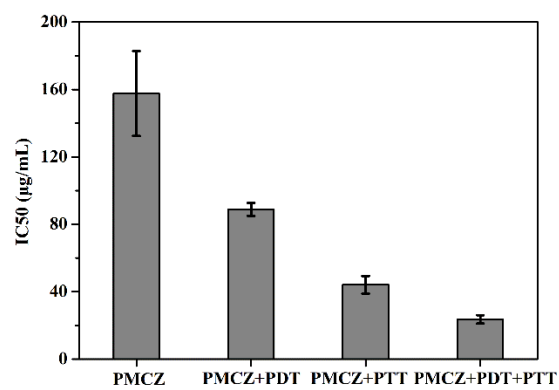


Fig. S10 IC50 values for the groups of the HeLa cells treated with various concentrations of nanomaterials. The plotting of the IC50 value for each group was calculated using SPSS software.

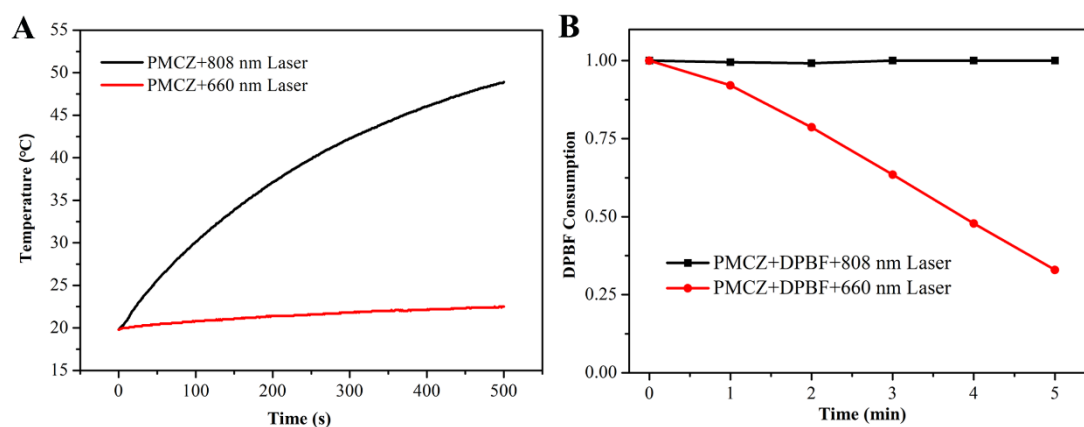


Fig. S11 (A) Temperature changes after irradiation (660 nm, 100 mW/cm² or 808 nm, 2 W/cm²) for different time in 1 mL of PBS containing PMCZ (50 µg/mL). (B) ¹O₂ production efficiency after irradiation (660 nm, 100 mW/cm² or 808 nm, 2 W/cm²) for different time in 1 mL of PBS containing PMCZ (50 µg/mL).

To validate feasibility of the system under 660 nm laser irradiation for PTT, 50 µg/mL of PMCZ was exposed to irradiation using 660 nm laser with a power density of 100 mW/cm² for 5 min, and the temperature increases of the sample were monitored as a function of laser irradiation time. Figure S11A showed that the temperature increased only several degrees, much lower than the temperature of the sample under 808 nm irradiation with a power density of 2 W/cm² for 5 min. The result indicated that the photothermal effect of PMCZ was insignificant, and the current system was not suitable for PTT under 660 nm laser irradiation.

To validate feasibility of the system under 808 nm laser irradiation for PDT, 1,3-diphenylisobenzofuran (DPBF) was employed as a ¹O₂ probe to evaluate the production of ¹O₂. Upon ¹O₂ oxidation, the intensity of the characteristic absorption of DPBF at around 410 nm would decrease. Under 808 nm laser with a power density of 2 W/cm² for 5 min, we found that 50 µg/mL of PMCZ induced negligible the generation of ¹O₂ (Figure S11B). The results indicated that the current system was not suitable for PDT under 808 nm laser irradiation.

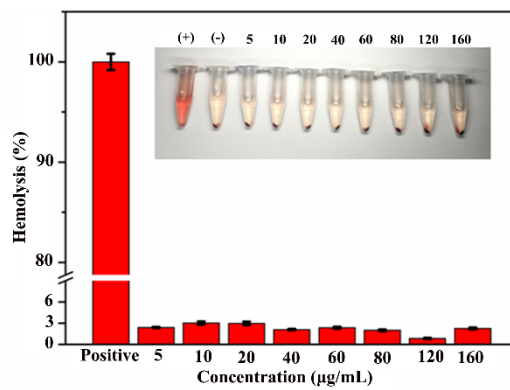


Fig. S12 Hemolytic activity of PMCZ as a function of concentration. Insert: photograph of hemolytic activity of PMCZ as a function of concentration.

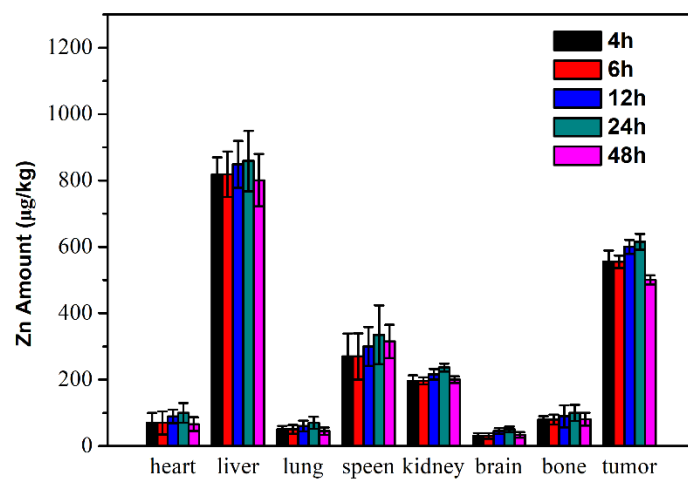


Fig. S13 Biodistribution of Zn after mice were injected with PMCZ (160 µL, 2 mg/mL) at different time points (4, 6, 12, 24, 48 h). The data were according to ICP-MS analysis of Zn contents from different organs.

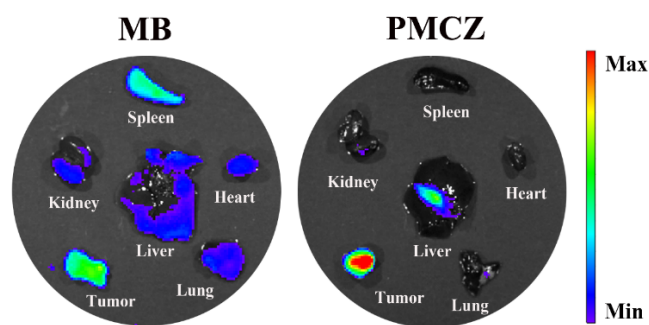


Fig. S14 *Ex vivo* fluorescence images of heart, liver, spleen, lung, kidney and tumor extracted from HeLa tumor-bearing mice treated with free MB and PMCZ (50 μ L, 800 μ g/mL). The tumor-bearing mice were sacrificed after intravenously injected with MB or PMCZ for 24 h, and the major organs were collected for imaging.

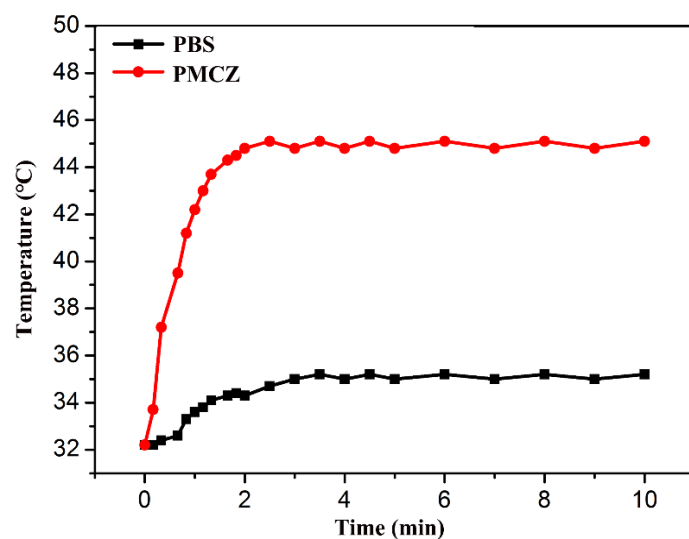


Fig. S15 Temperature curves of tumor sites in mice treated with PBS (50 μ L) or PMCZ (50 μ L, 800 μ g/mL) followed 808 nm laser irradiation for 10 min (1 W/cm²).

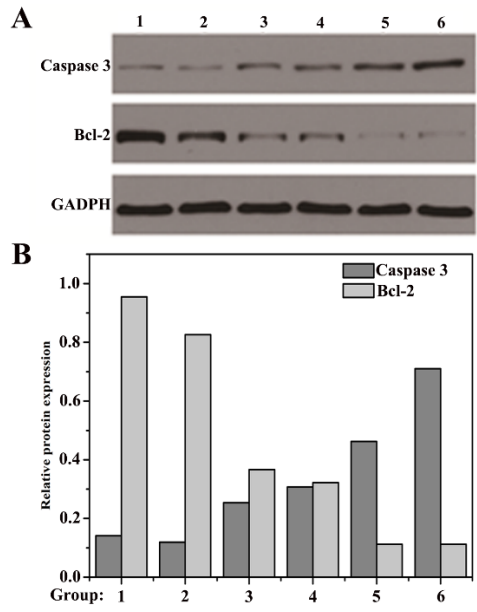


Fig. S16 (A) Western blot assay of caspase-3 and Bcl-2 protein expressions from tumors after different treatments. (B) The corresponding quantitative analysis of caspase-3 and Bcl-2 proteins in tumors after different treatments as determined by western blot assay.

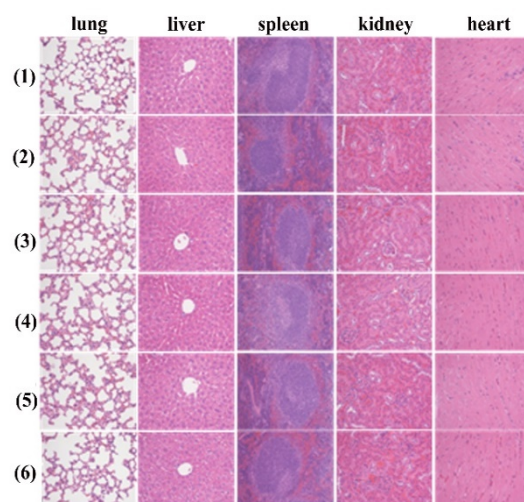


Fig. S17 Pathological H&E stained images of tissue sections from heart, liver, spleen, lung and kidney harvested from HeLa tumor-bearing mice on the 14th day treated with PBS (50 μL) (1), PMCZ (50 μL , 800 $\mu\text{g}/\text{mL}$) (2), PMCZ (50 μL , 800 $\mu\text{g}/\text{mL}$)+PDT (660 nm, 1 W/cm^2) (3), PMCZ (50 μL , 800 $\mu\text{g}/\text{mL}$)+PTT (808 nm, 1 W/cm^2) (4), PMZ (50 μL , 800 $\mu\text{g}/\text{mL}$)+PDT (660 nm, 1 W/cm^2)+PTT (808 nm, 1 W/cm^2) (5) and PMCZ (50 μL , 800 $\mu\text{g}/\text{mL}$)+PDT (660 nm, 1 W/cm^2)+PTT (808 nm, 1 W/cm^2) (6).

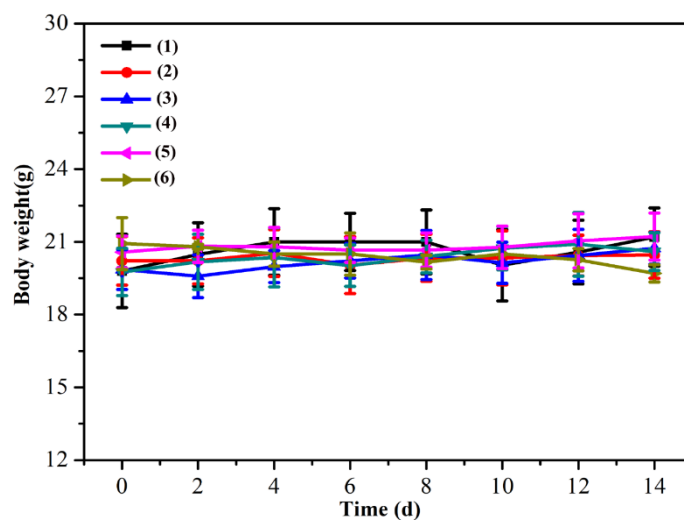


Fig. S18 Body weights of HeLa tumor-bearing mice after different treatments: PBS (50 μL) (1), PMCZ (50 μL , 800 $\mu\text{g}/\text{mL}$) (2), PMCZ (50 μL , 800 $\mu\text{g}/\text{mL}$)+PDT (660 nm, 1 W/cm^2) (3), PMCZ (50 μL , 800 $\mu\text{g}/\text{mL}$)+PTT (808 nm, 1 W/cm^2) (4), PMZ (50 μL , 800 $\mu\text{g}/\text{mL}$)+PDT (660 nm, 1 W/cm^2)+PTT (808 nm, 1 W/cm^2) (5) and PMCZ (50 μL , 800 $\mu\text{g}/\text{mL}$)+PDT (660 nm, 1 W/cm^2)+PTT (808 nm, 1 W/cm^2) (6).